Spherical Born Kernels for Flows in Time-Distance Helioseismology

Vincent Böning[1], Markus Roth[1], Wolfgang Zima[1], Aaron C. Birch[2], Laurent Gizon[2]

[1]Kiepenheuer-Institut für Sonnenphysik, Freiburg, Germany
[2]Max-Planck-Institut für Sonnensystemforschung, Göttingen, Germany

Abstract

We extend an existing Born approximation model for calculating the linear sensitivity of helioseismic travel-times to flows from Cartesian to spherical geometry. This development is necessary to use the Born approximation for inferring large-scale flows in the deep solar interior. Two consistency tests show that results for our sensitivity kernels agree with reference values to within a few percent. Consequently, we evaluate the impact of different data analysis filters on the kernels for a meridional travel-distance of 42 degrees. When mainly low-degree modes are used (roughly l < 70), the sensitivity is concentrated in deeper regions and it visually best resembles a ray-path like structure, otherwise the sensitivity is concentrated near the surface. Among the different low-degree filters used, we find the phase-speed filtered kernel to be best localized at depth.

Zero-Order Problem

We assume a spherically symmetric, non-rotating Sun without interior perturbative flows as given by Model S [1]. Solar oscillations are modeled by a damped and driven wave equation (see also [2] and [3]),

$$\mathscr{L}[\xi] = \mathbf{S}, \qquad \mathscr{L}[\xi(\mathbf{r},\omega)] \equiv \rho_0(-\omega^2 - 2\mathrm{i}\omega\Gamma + \mathscr{H})[\xi(\mathbf{r},\omega)], \tag{1}$$

where $\mathbf{S}(\mathbf{r},\omega)$ are stochastic sources, $\xi(\mathbf{r},\omega)$ is the oscillatory displacement at location $\mathbf{r}$ at frequency ω, $\mathscr{H}$ is the linear wave operator (Eq. 3.245 in [4]) , Γ describes damping, and ρ_0 denotes density.
The zero and first-order problems are solved using oscillation eigenfunctions $\xi^{lmn}(\mathbf{r})$, for which $\mathscr{H}[\xi^{lmn}(\mathbf{r})] = \omega_{ln}^2\ \xi^{lmn}(\mathbf{r})$ with eigenfrequencies ω_{ln}, and which were calculated with model S [1] and ADIPLS [5].

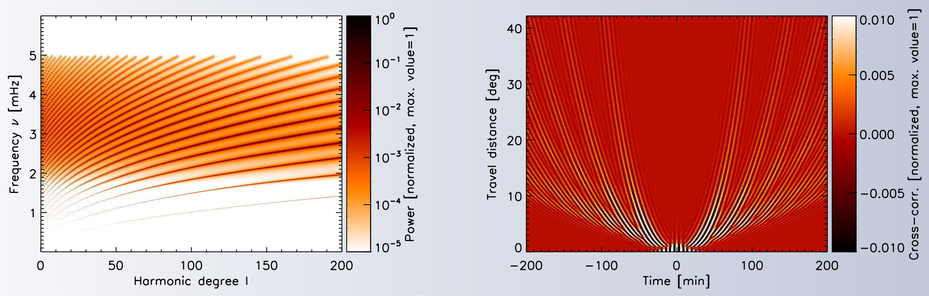

Figure 1: Example zero order power spectrum (left) and time-distance diagram (right), computed with the same specifications as for K_1, see Table 2, but with $l \leq 1000$ and with the same OTF as in Figure 2 in order to better match observations.

First-Order Problem and Spherical Kernels

The equation for the first-order (i.e., single-scattering) Born approximation to the perturbed wave equation in the presence of flows is, see [2],

$$(\mathscr{L} + \delta\mathscr{L})[\xi + \delta\xi] = \mathbf{S} + \delta\mathbf{S}. \tag{2}$$

We assume $\delta\mathbf{S} = \delta\Gamma = 0$ (see [6]). We also neglect the second order term $\delta\mathscr{L}[\delta\xi]$. Following [3], we assume that the perturbation to the wave operator is given by wave advection. Equation (2) is used to solve for the perturbative wave field in the presence of flows, $\delta\xi$, and to find a linear relation between the perturbation to the zero order cross-correlation, δC, and the flow $\mathbf{v}(\mathbf{r})$, using the perturbed line-of-sight projected and filtered Doppler signal produced by the wave field, $\Phi + \delta\Phi$,

$$\delta C(\mathbf{r}_1,\mathbf{r}_2,\omega) = \frac{2\pi}{T}\mathbb{E}\Big[\Phi^*\delta\Phi + \delta\Phi^*\Phi\Big] = \int_\odot \mathbf{v}(\mathbf{r})\cdot\mathscr{C}(\mathbf{r}_1,\mathbf{r}_2,\omega;\mathbf{r})\,\mathrm{d}^3\mathbf{r}. \tag{3}$$

Taking into account the effect of δC on the observed perturbed travel-times, $\delta\tau_{\text{diff}}$, through the fitting procedure (W), the sensitivity kernel $\mathbf{K}$ can be obtained from

$$\delta\tau_{\text{diff}}(\mathbf{r}_1,\mathbf{r}_2) = \int_{-\infty}^{\infty} W_{\text{diff}}(\mathbf{r}_1,\mathbf{r}_2,t)\,\delta C(\mathbf{r}_1,\mathbf{r}_2,t)\,\mathrm{d}t = \int_\odot \mathbf{K}(\mathbf{r}_1,\mathbf{r}_2;\mathbf{r})\cdot\mathbf{v}(\mathbf{r})\,\mathrm{d}^3\mathbf{r}. \tag{4}$$

In order to extend the code from Cartesian (see [3]) to spherical geometry, the eigenfunctions are written

$$\xi^{lmn}(\mathbf{r}) = \left[R_{ln}(r)\hat{\mathbf{e}}^{(r)} + \frac{H_{ln}(r)}{\sqrt{l(l+1)}}\left(\hat{\mathbf{e}}^{(\theta)}\partial_\theta + \frac{\hat{\mathbf{e}}^{(\phi)}}{\sin\theta}\partial_\phi\right)\right]Y_{lm}(\theta,\phi). \tag{5}$$

Sanity Check

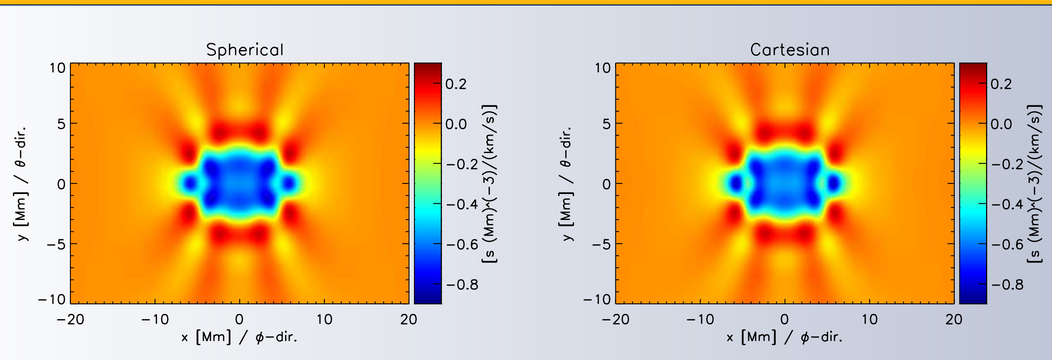

Figure 2: Horizontal cuts at the source depth through the sensitivity of travel-time differences to zonal flows, K_ϕ (left, spherical code) and K_x (right, from the Cartesian code used by [3]). The two observation points are located on the equator ($y = 0$) at $x = \pm 5\,\mathrm{Mm}$.

Kernel	$\max(K_\phi)$ $[\mathrm{s}^2/(\mathrm{Mm}^3\,\mathrm{km})]$	$\min(K_\phi)$ $[\mathrm{s}^2/(\mathrm{Mm}^3\,\mathrm{km})]$	$\int K_\phi\,\mathrm{d}^3\mathbf{r}$ $[\mathrm{s}/(\mathrm{m}/\mathrm{s})]$	$\min(\int K_\phi\,\mathrm{d}\Omega)$ $[\mathrm{s\,m}^{-1}/(\mathrm{m}/\mathrm{s})]$	ν_{mean} [mHz]	ν at max. int. power [mHz]
Fig. 2 in [3]	1.431	-4.421	-0.1887	-0.1067	2.77	2.70
Cartesian example	0.236	-0.848	-0.1193	-0.0446	2.55	2.41
Spherical example	0.233	-0.806	-0.1191	-0.0445	2.53	2.27

Table 1: Key Characteristics of Sanity Check Example Kernels

Conclusions:

(1) As a first **sanity check** of our newly developed spherical kernel code, we compute an example kernel the results of which are in **good accordance** with those from an existing Cartesian code [3].
(2) The kernels show a strong dependence on the underlying power spectrum: A change of $\delta\,\nu_{\text{mean}} = 0.2\,\mathrm{mHz}$ changed the mean sensitivity from $-0.1887\,\mathrm{s}/(\mathrm{m}/\mathrm{s})$ to $-0.1193\,\mathrm{s}/(\mathrm{m}/\mathrm{s})$, see Table 1.

Meridional Flow Example Kernels for $\Delta = 42°$

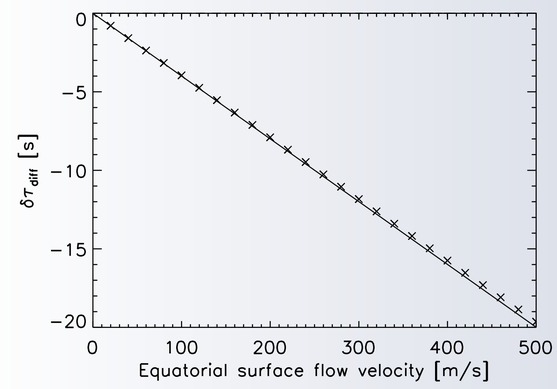

Figure 3: Perturbations to the travel-time difference as a function of the equatorial surface flow velocity in the case of uniform rotation. The observation points are assumed to be aligned in W-E direction on the equator at a distance of 42°. We show forward-modeled travel-time differences from the kernel (solid line) and from an analytical solution to the perturbed cross-correlation (crosses).

Kernel	Filter	mean l	mean ν [mHz]
K_1	$l \leq 170$	84	2.933
K_2	$l \leq 99$	49	2.929
K_3	$l \leq 79$	39	2.928
K_4	$l \leq 49$	24	2.927
K_5	Gaussian ($l_0 = 45$, $\delta l = 8$), $15 \leq l \leq 75$	45	2.928
K_6	phase-speed [7], $l \leq 170$	46	2.995

Table 2: Key Characteristics of $\Delta = 42°$ Example Kernels

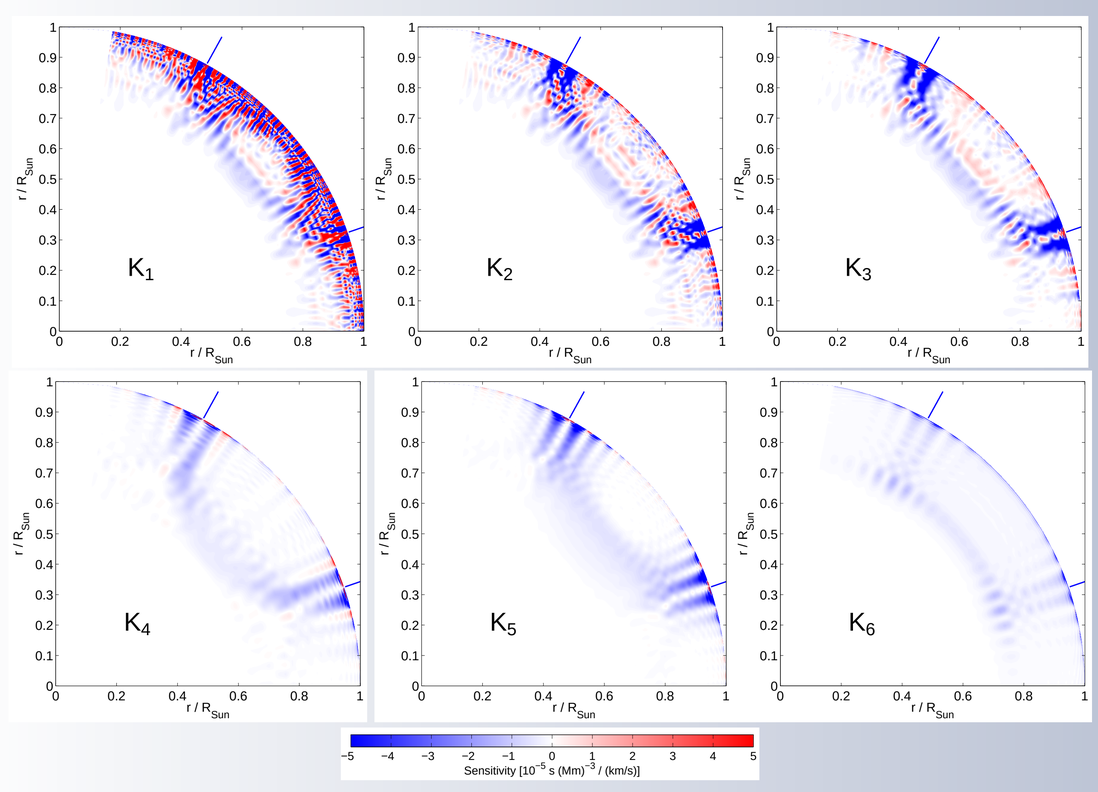

Figure 4: Vertical cuts at the central meridian through example travel-time sensitivity functions for meridional flow, K_θ, for a travel distance of $\Delta = 42°$. The locations of the observation points are marked with blue bars.

Conclusions:

(1) Total integrals of our spherical sensitivity kernels **agree** with reference values to within a few percent, see Figure 3.

Table 2 and Figure 4:
(2) The kernels show a strong dependence on the choice of data analysis filter.
(3) When using higher-degree modes (roughly $90 \lesssim l \lesssim 170$, K_1 and K_2), the sensitivity shows a large-valued ringing-like pattern near the surface.
(4) When lower-degree modes are used ($l \lesssim 70$), the sensitivity is concentrated in deeper regions and it visually best resembles a ray-path like structure.
(5) Among the different low-degree filters, the phase-speed filtered kernel is best localized at depth.

Summary

A newly developed model for computing spherical Born Approximation kernels for inferring large-scale flows in the solar interior using time-distance helioseismology is presented. Our method was succesfully tested and a number of consequences of the choice of data analysis filters on the kernels were evaluated (see conclusions above).
As a further consequence for interpreting observations, we note that travel times have to be interpreted with caution (see also, e.g., 8 and 9). The choice of filtering (not to filter is also a choice) may introduce significant differences in the kernels and the response may be sensitive to a small change in the set of modes used. It is an open question, however, how inversion results are affected by such changes in the kernels.

References

[1] J. Christensen-Dalsgaard, W. Dappen, S. V. Ajukov, E. R. Anderson, H. M. Antia, S. Basu, V. A. Baturin, G. Berthomieu, B. Chaboyer, S. M. Chitre, A. N. Cox, P. Demarque, J. Donatowicz, W. A. Dziembowski, M. Gabriel, D. O. Gough, D. B. Guenther, J. A. Guzik, J. W. Harvey, F. Hill, G. Houdek, C. A. Iglesias, A. G. Kosovichev, J. W. Leibacher, P. Morel, C. R. Proffitt, J. Provost, J. Reiter, E. J. Rhodes, Jr., F. J. Rogers, I. W. Roxburgh, M. J. Thompson, and R. K. Ulrich. The Current State of Solar Modeling. *Science*, 272:1286–1292, May 1996. doi: 10.1126/science.272.5266.1286.
[2] L. Gizon and A. C. Birch. Time-Distance Helioseismology: The Forward Problem for Random Distributed Sources. *Astrophys. J.*, 571:966–986, June 2002. doi: 10.1086/340015.
[3] A. C. Birch and L. Gizon. Linear sensitivity of helioseismic travel times to local flows. *Astronomische Nachrichten*, 328:228, March 2007. doi: 10.1002/asna.200610724.
[4] C. Aerts, J. Christensen-Dalsgaard, and D. W. Kurtz. *Asteroseismology*. 2010.
[5] J. Christensen-Dalsgaard. ADIPLS - the Aarhus adiabatic oscillation package. *Astrophys. Spa. Sci.*, 316:113–120, August 2008. doi: 10.1007/s10509-007-9689-z.
[6] J. Jackiewicz, L. Gizon, A. C. Birch, and T. L. Duvall, Jr. Time-Distance Helioseismology: Sensitivity of f-mode Travel Times to Flows. *Astrophys. J.*, 671:1051–1064, December 2007. doi: 10.1086/522914.
[7] S. Kholikov, A. Serebryanskiy, and J. Jackiewicz. Meridional Flow in the Solar Convection Zone. I. Measurements from GONG Data. *Astrophys. J.*, 784:145, April 2014. doi: 10.1088/0004-637X/784/2/145.
[8] K. DeGrave, J. Jackiewicz, and M. Rempel. Validating Time-Distance Helioseismology with Realistic Quiet-Sun Simulations. *Astrophys. J.*, 788:127, June 2014. doi: 10.1088/0004-637X/788/2/127.
[9] M. Švanda. Issues with time-distance inversions for supergranular flows. *A&A*, 575:A122, March 2015. doi: 10.1051/0004-6361/201425203.

Acknowledgements: The research leading to these results has received funding from the European Research Council under the European Union's Seventh Framework Programme (FP/2007-2013) / ERC Grant Agreement n. 307117.

Contact: Vincent Böning, vboening@kis.uni-freiburg.de